

CONFERENCE PROGRAM

EXHIBIT HALL & ACTIVITIES

REGISTER & PLAN TRAVEL

RESERVE EXHIBIT SPACE

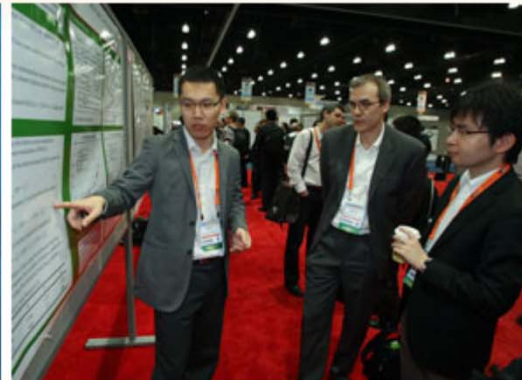
SUBMIT PAPERS

ABOUT OFC/NFOEC

The World's Leading Event for Advancing Optical Solutions in Telecom, Datacom, Computing and More

Are you in OFC/NFOEC's photo album?

Check out the photos from last year on our Flickr site.



[Learn About Registration Categories](#)

Select a category

discoverLosAngeles
LA INC. THE LOS ANGELES CONVENTION AND VISITORS BUREAU

[Plan My Itinerary](#)
[View Conference Program](#)

[Register Today](#)

[Book Housing](#)
with Travel Planners

[Read the OFC/NFOEC Blog](#)
[Bring Your Team](#)
[What's free at OFC/NFOEC?](#)

[Read Technical Attendee and Exhibits Pass Plus Testimonials](#)

11,000 of your colleagues will attend in March — You should too!

High Quality Science & Comprehensive Programming

- [Invited Presentations](#) given by experts in the field
- Peer-reviewed technical presentations
- Up-to-the-minute research presented in [Postdeadline Sessions](#)
- Variety of presentation formats
- [Short Courses](#) with a broad range of topic areas
- Notable [Plenary Session](#) features exceptional keynote speakers
- [Interactive Workshops and Panel Discussions](#)

Hot Topics – Watch Interviews with OFC/NFOEC's Organizers

Hot Topics for 2012–It's All Here!

- 100G and beyond
- Green networks
- Spatial multiplexing
- Coherent detection for high spectral efficiency
- Data center networking
- Wireline–wireless networking

Corporate Sponsors



Room 403A

4:00 PM–6:00 PM
OM3A • Impairment Compensation

Presider: Yi Cai; Huawei, USA

OM3A.1 • 4:00 PM

Nonlinearity Compensation via Spectral Inversion and Digital Back-Propagation: A Practical Approach, Danish Rafique¹, Andrew D. Ellis¹; ¹Photonic Systems Group, Tyndall National Institute, Ireland. We report performance enhancements enabled by pre-dispersed spectral inversion equivalent to that of ideal back-propagation, with further x2 increase in reach from multi-channel compensation, with spectral inversion employed upto 400km (from mid-link) with <1dB penalties.

OM3A.2 • 4:15 PM

Experimental Investigation on Non-linear Distortions with Perturbation Back-propagation Algorithm in 224 Gb/s DP-16QAM Transmission, Shoichiro Oda¹, Takahito Tanimura², Takeshi Hoshida¹, Yuichi Akiyama¹, Hisao Nakashima¹, Kyosuke Sone², Yasuhiko Aoki¹, Weizhen Yan³, Zhenning Tao³, Liang Dou³, Lei Li³, Jens C. Rasmussen¹, Yoshinori Yamamoto⁴, Takashi Sasaki⁵; ¹Fujitsu Limited, Japan; ²Fujitsu Laboratories Ltd., Japan; ³Fujitsu R&D Ctr. Co., Ltd., Japan; ⁴Sumitomo Electric Industries, Ltd., Japan. We investigate the impact of perturbation back-propagation algorithm on distribution of nonlinear noise in 224 Gb/s DP-16QAM transmission over large-Aeff pure silica core fiber and show the distribution approaches to Gaussian by the non-linear compensation.

Room 403B

4:00 PM–6:00 PM
OM3B • Quantum Information & Parametric Processing

Presider: Thomas Murphy; Univ. of Maryland, USA

OM3B.1 • 4:00 PM

Experimental Demonstration of All-Optical Modulation Format Conversion from NRZ-OOK to RZ-8APSK Based on Fiber Nonlinearity, Akihiro Maruta¹, Nozomi Hashimoto¹; ¹Communication Engineering, Osaka Univ., Japan. All-optical modulation format conversion scheme from 3-channels NRZ-OOK to RZ-8APSK based on nonlinearity in optical fiber is proposed and experimentally demonstrated. 3-channels 10.7Gb/s NRZ-OOK signals are converted to 32 Gb/s RZ-8APSK signal by XPM and optical parametric amplification.

OM3B.2 • 4:15 PM

Simultaneous Demultiplexing of OTDM Channels Based on Swept-Pump Fiber-Optical Parametric Amplifier, Chi Zhang¹, Xie Wang¹, Xing Xu¹, Po Ching Chui¹, Kenneth K. Y. Wong²; ¹Dept. of Electrical and Electronic Engineering, The Univ. of Hong Kong, Hong Kong. We experimentally demonstrate simultaneous demultiplexing of 80-Gb/s OTDM signal by transforming it into WDM idlers (spaced by 1.15 nm), based on a swept-pump fiber-optical parametric amplifier (FOPA), and ~10-dB parametric gain is achieved.

Room 406A&B

OFC

4:00 PM–5:30 PM
OM3C • Spatial Multiplexing & Amplification & Monitoring

Presider: Yoshinori Yamamoto; Sumitomo Electric Industries, Ltd., Japan

OM3C.1 • 4:00 PM

Wide-band error-free wavelength conversion based on continuous-wave-triggered supercontinuum, Xing Xu¹, Chi Zhang¹, T. i. Yuk¹, Kevin K. Tsia¹, Kenneth K. Y. Wong¹; ¹Electrical and Electronic Engineering, The Univ. of Hong Kong, Hong Kong. We demonstrate a wavelength converter based on CW-triggered picosecond supercontinuum (SC), with significantly enhanced spectrum over 300-nm. While error-free operations are obtained for wavelength converted signals from 1510 to 1615 nm.

OM3C.2 • 4:15 PM

Side-tap modal channel monitor for mode division multiplexed (MDM) systems, Lu Yan¹, Roman A. Barankov¹, Paul Steinvurzel¹, Siddharth Ramachandran¹; ¹Boston Univ., USA. We demonstrate a sidetap modal channel monitor based on a tilted Bragg grating, where different modes radiate at different angles. We qualitatively correlate the observed modal power partitioning with more accurate interferometer-based measurements.

Room 408A

4:00 PM–6:00 PM
OM3D • Fiber Fabrication and New Materials

Presider: Takashi Sasaki; Sumitomo Electric Industries, Japan

OM3D.1 • 4:00 PM Tutorial

Fiber Technologies: Materials and Processes, Ji Wang¹; ¹Corning Incorporated, USA, USA. This tutorial will review the requirement of key glass attributes and processes for optical fiber fabrication for both soft (multi-component) glasses, and high-silica based glasses. Examples will be given in each case on how the glass properties are tailored via composition and/or advanced processing for successful fiber optic applications.



Dr. Wang is currently the head of OVD fiber processing group and a Sr. Res. Associate at Corning. He received a Ph.D. in Optical Fiber Materials and Fiber Optics from the University of Southampton, England in 1993, and M.Sc. in Optics/Optical Materials from Changchun Institute of Optics, Fine Mechanics and Physics (CIOMP), Chinese Academy of Sciences, Changchun, China in 1985, and has been with Science and Technology Division, Corning Incorporated, Corning, New York, USA since 1998. He has researched and led many new optical fiber processing R&D projects, most notably on the fabrication of SBS-managed, Yb-doped double-clad high-

(continued on pg. 66)

Room 408B

4:00 PM–6:00 PM
OM3E • Photonic Integration

Presider: Liming Zhang; Bell Labs, Alcatel-Lucent, USA

OM3E.1 • 4:00 PM

A Hybrid Photonic Integrated Wavelength Converter on a Silicon-on-Insulator Substrate, Christos Stamatiadis¹, Leontios Stampoulidis², Konstantinos Vyroskinos¹, Ioannis Lazarou¹, Dimitris Kalavrouziotis¹, Lars Zimmermann^{3,4}, Karsten Voigt³, Giovanni Preve⁵, Ludwig Moerl⁶, Jochen Kreissl⁶, Hercules Avramopoulos¹; ¹ICCS/NTUA, Greece; ²Constelex Technology Enablers, Greece; ³Technische Universitaet Berlin, Germany; ⁴IHP GmbH, Germany; ⁵Nanophotonics Technology Ctr., Spain; ⁶Fraunhofer-Institut für Nachrichtentechnik, Germany. We present fabrication and testing of a wavelength converter integrated on a silicon-on-insulator substrate. The chip employs a hybrid integrated SOA and delay-interferometers integrated on 4µm SOI. We demonstrate 40Gb/s error-free performance.

OM3E.2 • 4:15 PM

A 12.5-Gb/s SiGe BiCMOS Optical Receiver with a Monolithically Integrated 850-nm Avalanche Photodetector, Jin-Sung Youn¹, Myung-Jae Lee¹, Kang-Yeob Park¹, Holger Rucker², Woo-Young Choi¹; ¹EE Engineering, Yonsei Univ., Republic of Korea; ²IHP, Germany. We demonstrate high-performance 850-nm SiGe BiCMOS Opto-Electronic Integrated Circuit (OEIC) receiver with Si avalanche photodetector. With the fabricated OEIC receiver, 12.5-Gb/s optical data are successfully detected with sensitivity of -7.5 dBm.

Room 409A&B

NFOEC

4:00 PM–6:00 PM
NM3F • Photonic Network Optimization

Presider: Jens Rasmussen; Fujitsu, Japan

NM3F.1 • 4:00 PM

Traffic Grooming in WDM Mesh Networks with Loop-Free Paths, Kwok Shing Ho¹, Victor Yu Liu²; ¹Huawei Technologies, China; ²Huawei Technologies, USA. A solution framework for the traffic grooming problem with physical loop-free end-to-end paths is proposed and its impacts in terms of network resource efficiency and installation cost is analyzed.

NM3F.2 • 4:15 PM

Quantifying the Impact of DWDM Nodes with Flexible Add/Drop Port Utilization for Dynamic Connection Setup, Joao Pedro^{1,2}, Silvia Pato^{1,3}; ¹Nokia Siemens Networks Portugal S.A., Portugal; ²Instituto de Telecomunicações, Instituto Superior Técnico, Portugal; ³Instituto de Telecomunicações, DEEC, Universidade de Coimbra, Portugal. DWDM transport networks are evolving towards dynamic setup/rerouting of optical connections. This paper quantifies the impact of optical node architecture and traffic variability on the network blocking probability and transponder count requirements.

A 12.5-Gb/s SiGe BiCMOS Optical Receiver with a Monolithically Integrated 850-nm Avalanche Photodetector

Jin-Sung Youn¹, Myung-Jae Lee¹, Kang-Yeob Park¹, Holger Rucker², and Woo-Young Choi¹

¹Department of Electrical and Electronic Engineering, Yonsei University, Seoul, Korea

²IHP, Im Technologiepark 25, 15236 Frankfurt (Oder), Germany

*Corresponding author: wchoi@yonsei.ac.kr

Abstract: We demonstrate high-performance 850-nm SiGe BiCMOS Opto-Electronic Integrated Circuit (OEIC) receiver with Si avalanche photodetector. With the fabricated OEIC receiver, 12.5-Gb/s optical data are successfully detected with sensitivity of -7.5 dBm.

OCIS codes: (250.1345) Avalanche photodiodes (APDs); (250.3140) Integrated optoelectronic circuits

1. Introduction

The required data rate for many short-distance interconnect applications (board-to-board, chip-to-chip, and within chip), is continuously and rapidly increasing. For example, the CPU-to-memory interface is expected to require 100 GB/s data transmission for multi/many core systems [1]. For these applications, existing copper-based electrical interconnects suffer from serious high-frequency losses, and optical interconnects are expected to play a crucial role. In order to realize optical interconnects in a cost-effective manner, various optical devices should be realized in Si technology and integrated with electronic circuits. As a part of such research efforts, several opto-electronic integrated circuit (OEIC) receivers based on Si technology have been reported [2–4]. In this paper, we demonstrate a 12.5-Gb/s 850-nm OEIC receiver with a silicon avalanche photodiode (Si APD) realized in standard SiGe BiCMOS technology without any process modification. We believe our OEIC receiver achieves the largest data rate with the smallest sensitivity as well as the smallest power consumption for Gb/s among Si OEIC receivers reported until now.

2. Opto-Electronic Integrated Circuit (OEIC) Receiver

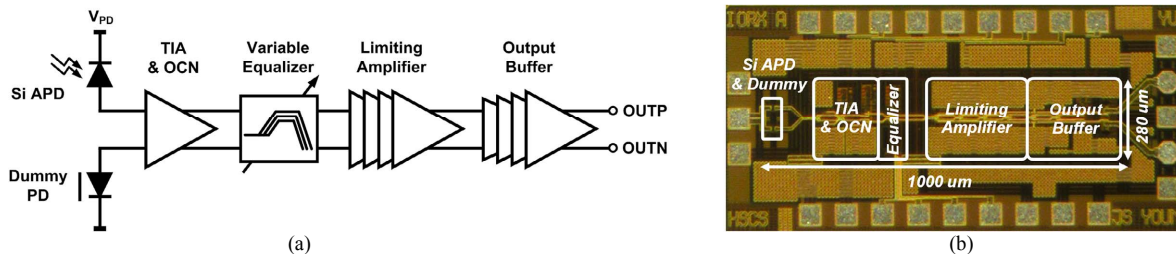


Fig. 1. (a) Simplified block diagram and (b) microphotograph of the fabricated OEIC receiver.

Fig. 1 (a) shows the simplified block diagram of our OEIC receiver realized in IHP's 0.25- μm SiGe BiCMOS technology. The technology provides high-speed performance in a cost-effective manner with CMOS-friendly integration scheme [5]. The OEIC receiver is composed of a Si APD with a dummy PD, a transimpedance amplifier (TIA), an offset cancellation network (OCN), an adaptive equalizer, a limiting amplifier, and an output buffer. Fig. 1 (b) shows the microphotograph of the fabricated receiver. The core chip size is about 1000 μm x 280 μm , and the power consumption of the electronic circuit excluding output buffer is about 59 mW with 2.5-V supply voltage.

Fig. 2 (a) shows the simplified cross-section view of the Si APD. It is realized by vertical P⁺/N-well junction having the active area of about 10 μm x 10 μm for optical window. The junction is surrounded by shallow trench isolation (STI) to alleviate premature edge breakdown. Fig. 2 (b) shows the measured current characteristics at different reverse bias voltages with and without optical illumination. The Si APD has avalanche breakdown voltage of about 12.3 V and low dark currents below a few nA below avalanche breakdown. As shown in Fig. 2 (c), the maximum responsivity and avalanche gain of the Si APD is about 12.98 A/W and 2400, respectively. Fig. 2 (d) shows the measured photodetection frequency response of the Si APD biased at 12.25 V. The 3-dB bandwidth is about 6 GHz. Details of device structure and characteristics of the Si APD can be found in [6,7].

Fig. 3 (a) shows the simplified block diagram for TIA and OCN. The shunt-feedback TIA is composed of two-stage differential amplifiers with feedback resistance of 3 k Ω . The pseudo-differential signal at TIA output due to

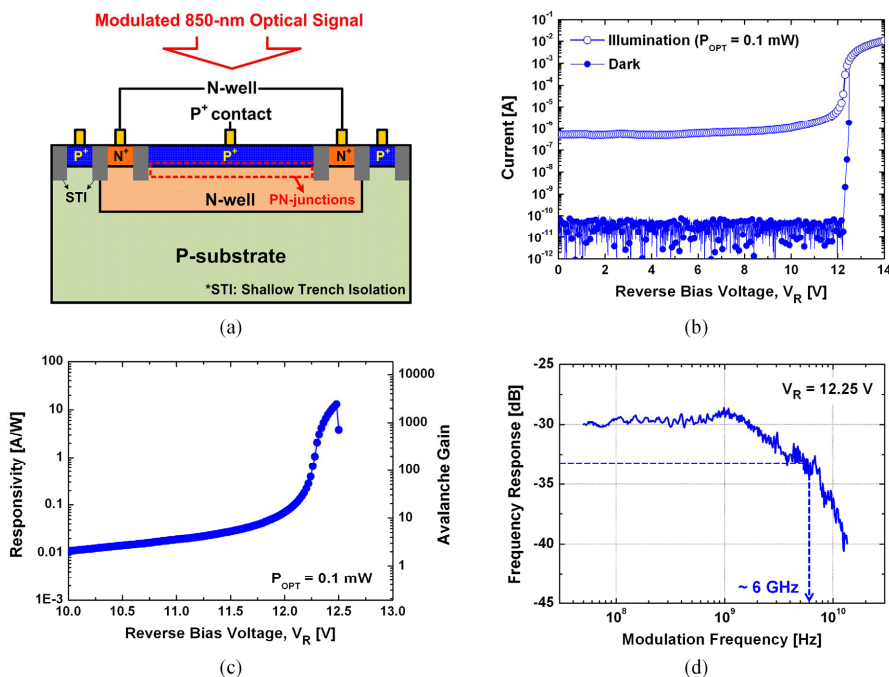


Fig. 2. (a) Cross-section view of the fabricated Si APD. (b) Measured current-voltage (I-V) characteristics. (c) Responsivity and avalanche gain. (d) Measured photodetection frequency response.

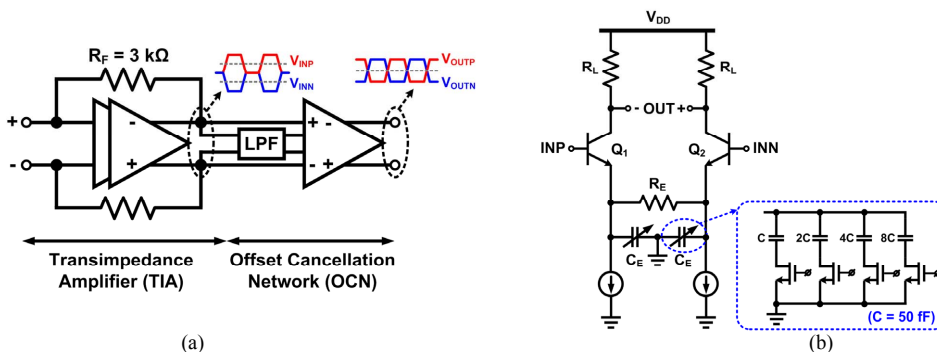


Fig. 3. (a) Simplified block diagram of the TIA and the OCN. (b) Schematic diagram of the variable equalizer with a capacitor array.

single-ended Si APD input is converted into fully differential by OCN, which consists of f_i -doubler amplifier and low-pass filter. Fig. 3 (b) shows the schematic diagram for the variable equalizer which compensates high-frequency losses due to the limited bandwidth of Si APD, TIA, and OCN. The equalizer is realized in differential configuration with emitter degeneration technique. In order to control high-frequency boosting gain of the variable equalizer, an emitter capacitor is composed of a 4-bit capacitor array. The equivalent emitter capacitance (C_E) can be digitally controlled from zero to 750 fF in steps of 50 fF by external switches. The limiting amplifier consists of 4 stages of identical gain cells, and each gain cell is composed of a differential amplifier with emitter degeneration. The output buffer is added for driving 50- Ω loads required for measurement.

3. Measurement Results

Photodetection frequency response and optical data detection experiment were performed on-wafer. An 850-nm laser diode and an external electro-optic modulator were used for generating modulated optical signals, which were transmitted through 4-m multimode fiber and injected into the fabricated OEIC receiver through a lensed fiber.

Fig. 4 (a) shows the measured photodetection frequency response of the OEIC receiver. The measured transimpedance gain and 3-dB bandwidth are about 110 dB Ω and 10 GHz, respectively, with $C_E = 400$ fF. By changing C_E , the 3-dB bandwidth can be tuned about 1 GHz. Fig. 4 (b) shows the bit-error rate (BER) as a function of injected optical power for 12.5-Gb/s 2⁷-1 pseudorandom bit sequence optical data. For this measurement, C_E was

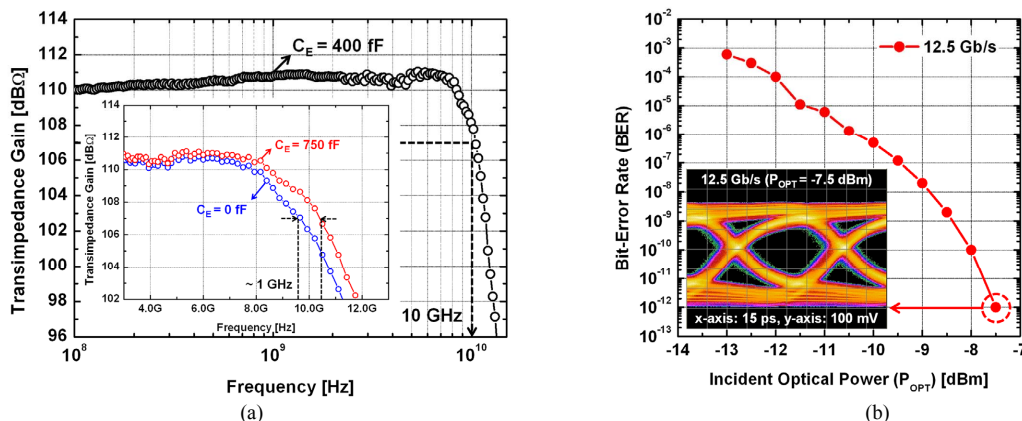


Fig. 4. (a) Measured photodetection frequency response and (b) measured BER performance of the fabricated OEIC receiver.

TABLE I
Comparison with the performance of the OEIC receiver fabricated with standard silicon technology

| | [2] JSSC | [3] JSSC | [4] JQE | This work |
|--------------------|-------------------------|--|-----------------------|-------------------------|
| Receiver Structure | SML*+TIA+EQ+LA | Meshed SML+TIA+LA (9 passive inductors) | APD+TIA+EQ+LA | APD+TIA+EQ+LA |
| Process | 0.13- μ m CMOS | 0.18- μ m CMOS | 0.13- μ m CMOS | 0.25- μ m BiCMOS |
| Maximum Data rate | 8.5 Gb/s | 10 Gb/s | 10 Gb/s | 12.5 Gb/s |
| Sensitivity (BER) | -3.2 dBm (10^{-12}) | -6 dBm (10^{-11}) | -4 dBm (10^{-12}) | -7.5 dBm (10^{-12}) |
| FOM [mW/Gb/s] | 5.53 | 11.8 | 6.68 | 4.72 |

*SML: Spatially-Modulated Light Detector

set at the optimal value of 400 fF. The optical sensitivity of our OEIC receiver is about -7.5 dBm for 10^{-12} BER. Inset of Fig. 4 (b) shows the corresponding eye diagram. For all of these measurements, the Si APD was biased at about 12 V provided by a separate power supply.

Table I compares recently-reported Si OEIC receivers fabricated with standard Si technology. Our receiver achieves the largest data rate with the smallest sensitivity. In addition, it has the smallest power consumption for Gbps.

4. Summary

A high-performance OEIC receiver is realized with standard 0.25- μ m SiGe BiCMOS technology. With the fabricated OEIC receiver, detection of 12.5-Gb/s optical data is successfully achieved with BER of 10^{-12} at incident optical power of -7.5 dBm. We expect our OEIC receiver will be very useful for 850-nm optical interconnect applications.

Acknowledgement

This work was supported by Mid-career Research Program through NRF grant funded by the MEST [2010-0014798]. The authors are very thankful to IC Design Education Center (IDEC) for EDA software support.

- [1] E. Mohammed, A. Alduino, T. Thomas, H. Braunisch, D. Lu, J. Heck, A. Liu, I. Young, B. Barnett, G. Vandentop, and R. Mooney, "Optical interconnect system integration for ultra-short-reach applications," *Intel Technol. J.*, vol. 8, no. 2, pp. 115–127, May 2004.
- [2] D. Lee, J. Han, G. Han, and S. M. Park, "An 8.5-Gb/s fully integrated CMOS optoelectronic receiver using slope-detection adaptive equalizer," *IEEE J. Solid-State Circuits*, vol. 45, no. 12, pp. 2861–2873, Dec. 2010.
- [3] S.-H. Huang, W.-Z. Chen, Y.-W. Chang, and Y.-T. Huang, "A 10-Gb/s OEIC with meshed spatially-modulated photo detector in 0.18- μ m CMOS technology," *IEEE J. Solid-State Circuits*, vol. 46, no. 5, pp. 1158–1169, May 2011.
- [4] J.-S. Youn, M.-J. Lee, K.-Y. Park, and W.-Y. Choi, "A 10-Gb/s 850-nm CMOS OEIC receiver with a silicon avalanche photodetector," *IEEE J. of Quantum Electron.*, to be published.
- [5] B. Heinemann, R. Barth, D. Knoll, H. Rucker, B. Tillack, and W. Winkler, "High-performance BiCMOS technologies without epitaxially-buried subcollectors and deep trenches," *Semiconductor Science and Technol.*, vol. 22, no. 1, pp. 153–157, Jan. 2007.
- [6] H.-S. Kang, M.-J. Lee, and W.-Y. Choi, "Si avalanche photodetectors fabricated in standard complementary metal-oxide-semiconductor process," *Appl. Phys. Lett.*, vol. 90, no. 15, pp. 151118-1–151118-3, Apr. 2007.
- [7] M.-J. Lee, H.-S. Kang, and W.-Y. Choi, "Equivalent circuit model for Si avalanche photodetectors fabricated in standard CMOS process," *IEEE Electron Device Lett.*, vol. 29, no. 10, pp. 1115–1117, Oct. 2008.